frontiers | Frontiers in Chemistry

TYPE Original Research
PUBLISHED 19 December 2022
DOI 10.3389/fchem.2022.1079214

OPEN ACCESS

EDITED BY
Weijie Zhang,
University of Virginia, United States

REVIEWED BY
Fanji Kong,
University of Virginia, United States
Zhou Lu,
University of North Texas, United States
Bo Zhang,
University of Nebraska-Lincoln, United States

*CORRESPONDENCE
Chih-Wei Tang,
cwtang@aaroc.edu.tw
Chen-Bin Wang,
chenbinwang@gmail.com

SPECIALTY SECTION
This article was submitted to Catalytic Reactions and Chemistry, a section of the journal Frontiers in Chemistry

RECEIVED 25 October 2022
ACCEPTED 05 December 2022
PUBLISHED 19 December 2022

CITATION
Tang C-W, Liu C-H, Yu S-W and Wang C-B (2022), Effect of support on the performance of PtRu-based catalysts in oxidative steam reforming of ethanol to produce hydrogen. *Front. Chem.* 10:1079214. doi: 10.3389/fchem.2022.1079214

Effect of support on the performance of PtRu-based catalysts in oxidative steam reforming of ethanol to produce hydrogen

Chih-Wei Tang[1]*, Chiu-Hung Liu[2], Shen-Wei Yu[3] and Chen-Bin Wang[3,4]*

[1]Department of General Education, Army Academy ROC, Taoyuan, Taiwan, [2]Graduate School of National Defense Science, Chung Cheng Institute of Technology, National Defense University, Taoyuan, Taiwan, [3]Department of Chemical and Materials Engineering, Chung Cheng Institute of Technology, National Defense University, Taoyuan, Taiwan, [4]Undergraduate Degree Program of System Engineering and Technology, National Yang Ming Chiao Tung University, Hsinchu, Taiwan

Oxidative steam reforming of ethanol (OSRE) to produce hydrogen has been investigated over a series of supported PtRu catalysts, with different supports. Bimetallic PtRu-based catalysts were prepared by the impregnation method using H_2PtCl_6 and $RuCl_3$ as precursors. Six supports (reducible oxides of ZrO_2, CeO_2, and Co_3O_4, and irreducible oxides of ZnO, Al_2O_3, and NiO) were chosen to fabricate bimetallic catalysts. The catalytic performance of the OSRE reaction in the series of PtRu-based samples was evaluated using a fixed-bed flow reactor under atmospheric pressure. In front reaction, the catalyst was pre-activated by reduction under 200°C for 3 h. The gas hourly space velocity was adjusted at 66,000 h^{-1}, and the optimal molar ratios of the H_2O/EtOH and O_2/EtOH feeds were 4.9 and 0.44, respectively. The results indicated that the PtRu supported on the ZrO_2 and CeO_2 exhibited superior catalytic performance in the OSRE reaction under a low temperature (a T_R of approximately 320°C) for producing the main products of H_2 and CO_2 with lower CO and CH_4 by-products. Also, it was quite stable during a long time evaluation; the maximum Y_{H2} maintained at 4.5–4.2, and the CO distribution approached 3.3–3.5 mol% around 84 h test at 340°C over the PtRu/ZrO_2 catalyst.

KEYWORDS

oxidative steam reforming of ethanol, H2 production, ZrO2, CeO2, PtRu-based based catalysts, support effect

1 Introduction

Hydrogen is a versatile element that is often used as a raw material for gasoline (the processes of hydrotreating and hydrocracking), chemistry (the synthesis of NH_3 and CH_3OH), foodstuff processing (hydrogenation of fats and oils), steel, and the manufacturing of electronics (Ramachandran and Menon, 1998; Armor, 1999).

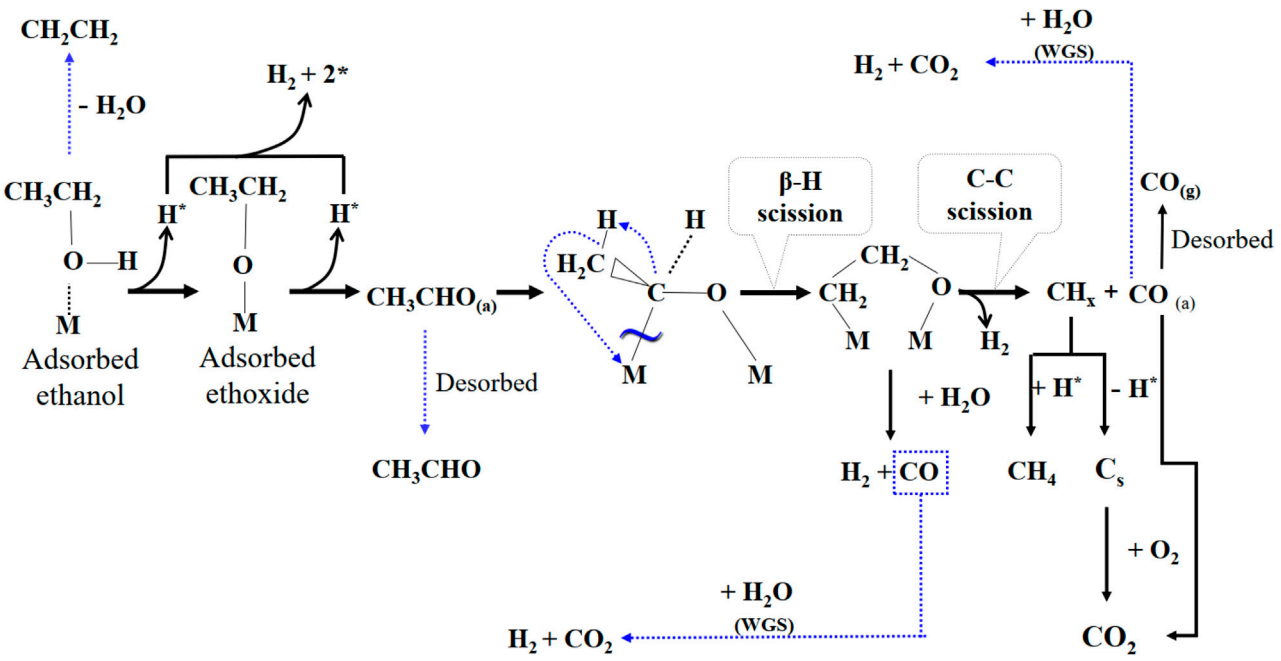

SCHEME 1
Reaction pathway for the OSRE reaction over the PtRu-based catalysts.

However, current industry does not produce hydrogen as an energy carrier or as a fuel for generators. In order to support sustainable global economic growth as well as reduce air pollution and the greenhouse effect, it is urgent to adopt hydrogen as an energy carrier; however, several technical hurdles must be conquered to manufacture and transfer the amount of hydrogen needed to reach a hydrogen-based economy.

Hydrogen can be manufactured from oxygenates, such as various ethanol reforming processes (Goldemberg, 2007; Ni et al., 2007; de la Piscina and Homs, 2008; Rabenstein and Hacker, 2008; Zanchet et al., 2015; Li et al., 2016) including the partial oxidation of ethanol (POE), steam reforming of ethanol (SRE), and oxidative steam reforming of ethanol (OSRE). The OSRE reaction is the incorporation of partial oxidation and steam reforming processes. Moreover, the OSRE reaction can lessen the energy of the SRE process and lower the rate of coke formation. Thermodynamic analysis of the production of hydrogen from ethanol by catalytic processes has found that the OSRE process possesses many advantages in terms of heat management and reforming efficiency (Rabenstein and Hacker, 2008).

Besides choosing a single active component (a noble or non-noble metal) as the reforming catalyst, multi-component catalysts have been reported in various catalytic reactions (Bi et al., 2007a; Alayoglu et al., 2008; Pereira et al., 2008; Koh et al., 2009; Pereira et al., 2010). Pereira et al. (Pereira et al., 2010) stated that the K-promoter enhances the catalytic behavior of CoRh/CeZr under the OSRE process to produce hydrogen, in which the addition of Rh facilitates the reducibility of Co. and enhances the catalytic activity. The same group also reported the effect of adding Ru and Rh to the $Co./SiO_2$ catalysts and found a

TABLE 1 Surface area and metal content of series PtRu-based catalysts.

Catalyst	S_{BET} ($m^2 \cdot g^{-1}$)	Metal content (wt%)	
		Pt	Ru
$PtRu/ZrO_2$	116	1.36	1.28
$PtRu/CeO_2$	104	1.38	1.34
$PtRu/Co_3O_4$	86	1.31	1.26
$PtRu/Al_2O_3$	131	1.41	1.38
PtRu/ZnO	58	1.34	1.33
PtRu/NiO	92	1.39	1.42

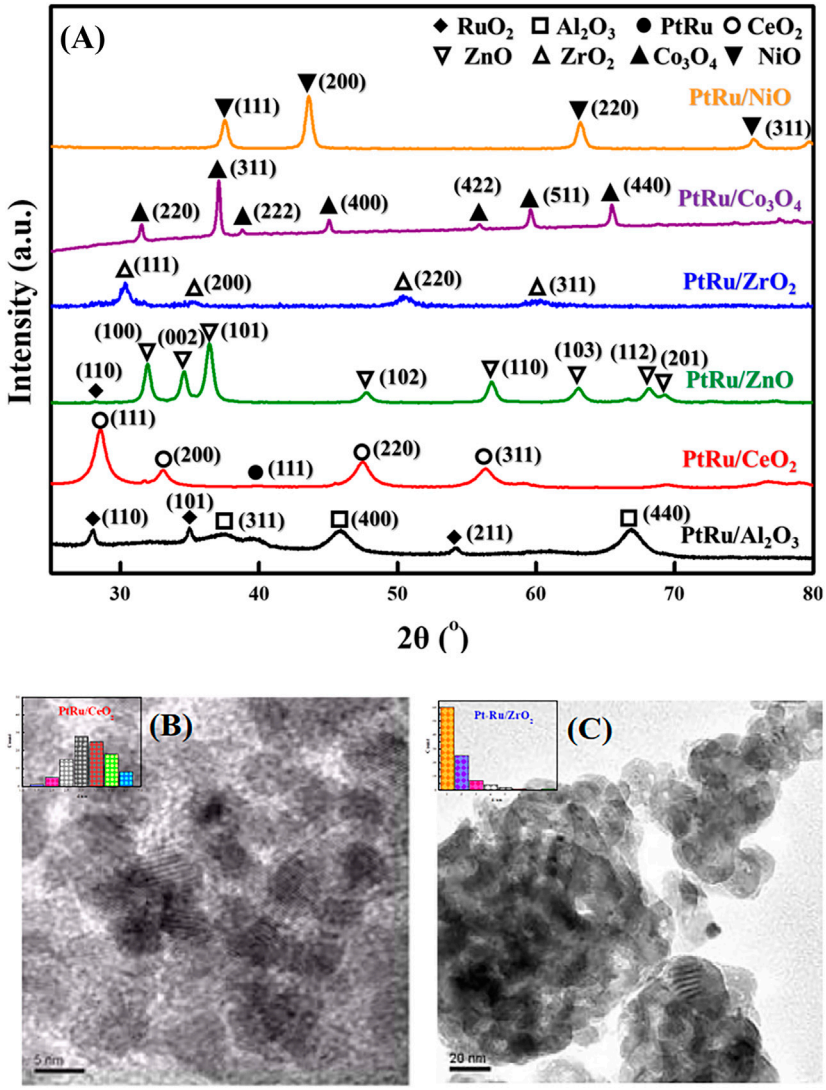

FIGURE 1
XRD patterns and TEM images of series PtRu-based catalysts: **(A)** XRD profile **(B)** TEM image of $PtRu/CeO_2$ catalyst **(C)** TEM image of $PtRu/ZrO_2$ catalyst.

synergistic effect between Co and Ru (or Rh) in the OSRE reaction (Pereira et al., 2008). In particular, bimetallic PtRu catalysts have been widely used as CO tolerant for polymer electrolyte fuel cells (PEFCs) (Alayoglu et al., 2008). An investigation on the catalytic ability of PtRu-based catalysts for hydrogen production in reforming reactions confirmed that $PtRu/ZrO_2$ is an excellent catalyst for low temperature OSRE reaction (Bi et al., 2007a). A nano-sized $PtRu/Al_2O_3$ originated from the organometallic clusters, which exhibited a high capability to manufacture hydrogen under the SRE reaction (Koh et al., 2009).

The performance of OSRE not only depends on the active metals; the other key factor is the nature of the support. To enhance the catalytic behavior of supported metal catalysts, support has influenced the catalytic performance (Llorca et al., 2002; Furtado et al., 2009; Youn et al., 2010; Wang and Spivey, 2015; Zhang et al., 2015; Tóth et al., 2016; Hsia et al., 2019). The effect of the support's (ZnO, MgO, ZrO_2, TiO_2, and Al_2O_3) acidity on the OSRE activity of supported nickel catalysts was explored by Youn et al. (Youn et al., 2010), in which the intermediate acidity of $Ni/Ti_{0.2}Zr_{0.8}O_2$ was identified as the optimal catalyst. The evaluation of the support materials (Al_2O_3, Nb_2O_5, and $Ce_{0.6}Zr_{0.4}O_2$) of a bimetallic NiCu-based catalyst on the SRE reaction showed that the $NiCu/Ce_{0.6}Zr_{0.4}O_2$ could achieve the best performance for hydrogen production (Furtado et al., 2009).

In our previous work, a $PtRu/ZrO_2$ catalyst modified with Na in an OSRE indicates active at 300°C and begets little CO at 340°C

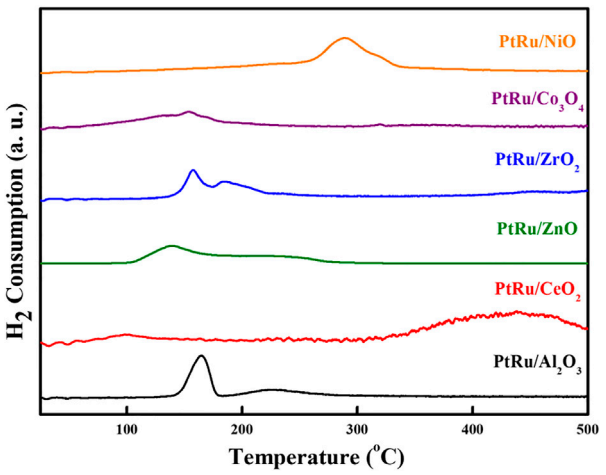

FIGURE 2
TPR profiles of series PtRu-based catalysts.

(Wang et al., 2011). Here in, the OSRE reaction was further studied over series PtRu-based catalysts. Six supports (reducible oxides of ZrO_2, CeO_2, and Co_3O_4, and irreducible oxides of ZnO, Al_2O_3, and NiO) were picked to fabricate supported bimetallic catalysts. The goal of this effort was to find an excellent and durable catalyst that could be applied to the on-board reforming of ethanol at low temperatures.

2 Experimental

2.1 Preparation of catalysts

Six supports (ZrO_2, CeO_2, Co_3O_4, ZnO, Al_2O_3, and NiO) were chosen to prepare the supported bimetallic catalysts. The Al_2O_3 was purchased from Merck (γ-form, 142 $m^2 \cdot g^{-1}$), while the others were self-synthesized. The ZrO_2 (130 $m^2 \cdot g^{-1}$) was prepared using the sol-gel method (Bi et al., 2007a), the CeO_2 (106 $m^2 \cdot g^{-1}$) was prepared using a simple reduction-oxidation method (Siang et al., 2010), the Co_3O_4 (102 $m^2 \cdot g^{-1}$) and NiO (104 $m^2 \cdot g^{-1}$) were prepared by the precipitation-oxidation method (Wang et al., 2005a; Lai et al., 2006), and the ZnO (89 $m^2 \cdot g^{-1}$) was obtained through the thermal decomposition of $Zn(OH)_2 \cdot 2ZnCO_3 \cdot xH_2O$ (Stream) in the air (Chiou et al., 2012), respectively. The supported PtRu catalysts were prepared by the impregnation method using an aqueous solution of H_2PtCl_6 (Merck) and $RuCl_3$ (Strem) as precursors (the loading of each component was 1.5 wt%). The as-prepared sample went through drying at 110°C and calcination at 400°C for 4 h in the air, after which the fabricated samples were smashed to 60–80 mesh and kept as fresh catalysts (both metal content and surface area are listed in Table 1).

2.2 Physicochemical characterizations

Both the Pt and the Ru contents in the fresh catalysts were ascertained by the measurement of ICP-MS (Perkin-Elmer). The surface area (S_{BET}) was measured with the physisorption using a Micromeritics ASAP 2010 instrument. First, the catalysts were pre-outgassed in a vacuum for 3 h at 110°C, then, the S_{BET} was measured by the N_2 adsorption at 77 K. The phases and crystalline structures were surveyed with X-ray diffraction (XRD) using a MAC Science MXP18 diffractometer with Cu $K_{\alpha 1}$ radiation (λ = 1.5405 Å) at 30 mA and 40 kV. The particle size was observed using transmission electron microscopy (TEM) images from a JEM-2010 transmission electron microscope (JEOL) with a 200 kV acceleration voltage. During the TPR experiment, a 50 mg sample located in the reactor and was heated at a ramping rate of 7°C·min^{-1} from RT to 500°C

TABLE 2 Effect of O_2/EtOH for OSRE reaction with various temperatures over the PtRu/ZrO_2 catalyst under a molar ratio of H_2O/EtOH = 4.9.

O_2/EtOH	T_R (°C)	Ethanol conversion (X_{EtOH}, %)/Products distribution (mol%)					Y_{H2}
		X_{EtOH}	H_2	CH_4	CO	CO_2	
0.32	280	100	47.6	12.1	16.7	23.6	1.8
	300	100	47.1	13.3	16.1	23.5	1.8
	320	100	46.7	15.4	15.5	22.4	1.8
0.44	280	100	64.1	2.3	11.0	22.6	3.3
	300	100	64.9	3.4	8.6	23.1	3.4
	320	100	71.4	1.2	3.4	24.0	4.2
0.61	280	100	60.3	6.9	12.1	20.7	2.1
	300	100	63.0	4.2	9.5	23.3	2.8
	320	100	63.4	2.4	10.6	23.6	2.9

TABLE 3 Effect of H_2O/EtOH for OSRE reaction with various temperatures over the PtRu/ZrO_2 catalyst under a molar ratio of O_2/EtOH = 0.44.

H_2O/EtOH	T_R (°C)	Ethanol conversion (X_{EtOH}, %)/Products distribution (mol%)					Y_{H2}
		X_{EtOH}	H_2	CH_4	CO	CO_2	
13	280	100	66.7	0	10.8	22.5	2.5
	300	100	66.8	0	10.7	22.5	2.9
	320	100	66.7	0	10.1	23.2	3.0
4.9	280	100	64.1	2.3	11.0	22.6	3.3
	300	100	64.9	3.4	8.6	23.1	3.4
	320	100	71.4	1.2	3.4	24.0	4.2
2.2	350	100	57.9	14.8	8.1	19.2	2.1
	370	100	60.1	16.0	7.8	16.1	2.2
	390	100	60.3	16.7	3.9	19.1	2.4
0.8	350	100	60.5	13.9	3.7	21.9	2.6
	370	100	61.2	18.5	3.5	16.8	2.2
	390	100	61.6	20.1	5.5	12.8	1.9

under a reducing gas (10% H_2/N_2) with a flow rate of 10 ml·min^{-1}. The consumption of H_2 was detected continuously using a thermal conductivity detector (TCD).

2.3 Activity test of catalysts

A fixed-bed flow reactor was chosen to evaluate the performance of the PtRu-based catalysts towards the OSRE reaction under atmospheric pressure. A 100-mg sample was placed in a quartz tubular reactor (4 mm i. d.) and guarded with glass-wool plugs. The reactor was twined with heating tape and the temperature was controlled using a thermocouple (1.2 mm i. d.) placed in the center of the reactor bed. Prior to the reaction, the catalyst was pre-activated by reduction at 200°C for 3 h. The catalytic activity of the series of supported PtRu catalysts towards OSRE was executed by tuning the molar ratio of the H_2O/EtOH (0.8–13) and O_2/EtOH (0.32–0.61), which was executed between 280°C and 600°C under atmospheric pressure. The outlet gas was detected by both gas chromatography (GC), one with an MS-5A column (for the separation of H_2, O_2, CH_4, and CO), and the other with a Porapak Q column (for the separation of C_2H_5OH, H_2O, CH_3CHO, $CH_3COOC_2H_5$, and CO_2). Based on the ethanol conversion (X_{EtOH}), selectivity of carbon monoxide (S_{CO}) and yield of hydrogen (Y_{H2}) to evaluate the catalytic performance as follows:

$$X_{EtOH}(\%) = \left[n(EtOH)_{in} - n(EtOH)_{out}\right] / n(EtOH)_{in} \times 100\% \quad (1)$$

$$S_{CO}(\%) = n(CO)_{out} / \left[n(CH_4)_{out} + n(CO)_{out} + n(CO_2)_{out}\right] \times 100\% \quad (2)$$

$$Y_{H2} = n(H_2)_{out} / \left[n(EtOH)_{in} - n(EtOH)_{out}\right] \quad (3)$$

3 Results and discussion

3.1 Characterization of catalysts

Figure 1A indicates the XRD patterns of the six bimetallic PtRu catalysts. Except for the PtRu/Al_2O_3 and PtRu/ZnO catalysts, which exhibited a very faint RuO_2 phase, no significant diffraction peak of PtRu (111) was observed in all catalysts. This result demonstrated that the nanoparticles of the bimetallic PtRu were smaller than 5 nm. The crystal phase of metal oxides is conspicuous, i.e. the unique diffraction peaks of PtRu/NiO at 37.6°, 43.6°, 63.2°, and 75.7°, corresponding to the (111), (200), (220) and (311) planes, respectively, were attributed to the cubic NiO (JCPDS 04-0835); the clear diffraction peaks of PtRu/Co_3O_4 at 31.5°, 37.1°, 38.8°, 45.1°, 55.9°, 59.6° and 65.5°, corresponding to the (220), (311), (222), (400), (422), (511) and (440) planes, respectively, were ascribed to the spinel Co_3O_4 (JCPDS 43-1003); the noticeable diffraction peaks of PtRu/ZrO_2 at 30.4°, 35.4°, 50.4° and 60.4°, corresponding to the (111), (200), (220) and (311) planes, respectively, were associated with the tetragonal ZrO_2 (JCPDS 79-1769); the distinct diffraction peaks of PtRu/ZnO at 31.9°, 34.6°, 36.4°, 47.8°, 56.8°, 63.1°, 68.2° and 69.3°, corresponding to the (100),

TABLE 4 Catalytic performance in the OSRE reaction over series PtRu-based catalysts under O_2/EtOH = 0.44 and H_2O/EtOH = 4.9.

Catalyst	TR(C)	Ethanol conversion (X_{EtoH}, %)/Products distribution (no! %)							Y_{H2}
		X_{E011}	H_2	CH_4	CO	CO_2	CH_2CH_2	CH_3CHO	
$PtRu/ZrO_2$	280	100	64.1	2.3	11.0	22.6			3.3
	300	100	64.9	3.4	8.6	23.1			3.4
	320	100	71.4	1.2	3.4	24.0			4.2
	340	100	71.7	1.1	3.3	23.9			4.5
$PtRu/CeO_2$	290	100	66.4	6.6	3.1	23.9			3.2
	320	100	68.4	5.5	2.8	23.3			3.5
	340	100	70.0	4.0	2.8	23.2			4.0
	360	100	68.7	5.0	2.5	23.8			3.8
$PtRu/Co_3O_4$	320	100	63.7	9.5	4.0	22.8			1.6
	340	100	67.4	6.8	2.6	23.2			3.1
	360	100	68.1	5.8	2.3	23.8			3.1
	380	100	69.5	5.1	2.6	23.8			2.9
$PtRu/Al_2O_3$	300	95	58.4	8.3	8.7	22.4	2.2		1.7
	375	96	58.7	11.8	5.4	23.1	1.0		1.8
	450	97	61.3	11.5	2.9	24.0	0.3		2.5
	500	97	65.0	9.2	1.4	24.4	0		2.8
PtRu/ZnO	300	93	53.3	10.6	8.7	23.2		4.2	1.4
	310	95	55.0	10.1	9.4	23.0		4.5	1.3
	500	96	54.2	15.2	6.0	23.7		3.9	1.5
	600	98	57.5	14.6	3.9	23.0		1.0	2.9
PtRu/NiO	400	98	65.3	5.3	3.4	23.0		3.0	3.0
	450	98	65.1	6.4	4.2	22.0		2.3	3.4
	500	98	67.9	4.6	2.8	23.5		1.2	4.4
	600	99	64.3	4.4	9.4	21.9		0	2.9

(002), (101), (102), (110), (103), (112) and (201) planes respectively, were well indexed to the hexagonal ZnO (JCPDS 79-2205); the bright diffraction peaks of PtRu/CeO_2 at 28.5°, 33.1°, 47.5° and 56.4° corresponding to the (111), (200), (220) and (311) planes, respectively, were confirmed the cubic CeO_2 (JCPDS 34-0394); the bright diffraction peaks of PtRu/Al_2O_3 at 37.3°, 45.9° and 66.9°, corresponding to the (311), (400) and (440) planes, respectively, were assigned to the γ-Al_2O_3 (JCPDS 10-0425). Figures 1B, C present the TEM images of the PtRu/CeO_2 and PtRu/ZrO_2, in which the average particle sizes of the PtRu were around 3.3 and 1.7 nm for both catalysts, respectively. The reducibility of the bimetallic PtRu catalysts was evaluated using temperature programmed reduction experiments (the TPR profile is listed in Figure 2). According to the literature (Trovarelli, 1996; Lin et al., 2003; Wang et al., 2005a; Wang et al., 2005b; Lai et al., 2006; Siang et al., 2010), the reduction of NiO occurs around 300°C (Wang et al., 2005b; Lai et al., 2006), the reduction of Co_3O_4 occurs around 200–400°C (Lin et al., 2003; Wang et al., 2005a), and the reduction of the surface capping oxygen ions of CeO_2 occurs above 400°C (Trovarelli, 1996; Siang et al., 2010). The results showed that in addition to the reduction of the active species (the bimetallic oxide reduced at below 200°C for all catalysts and the RuO_2 reduced at around 200°C–300°C for the PtRu/Al_2O_3 and PtRu/ZnO catalysts) (Bi et al., 2007a), the NiO, Co_3O_4, and the surface oxygen of the CeO_2 supports could also be reduced at temperatures below 500°C.

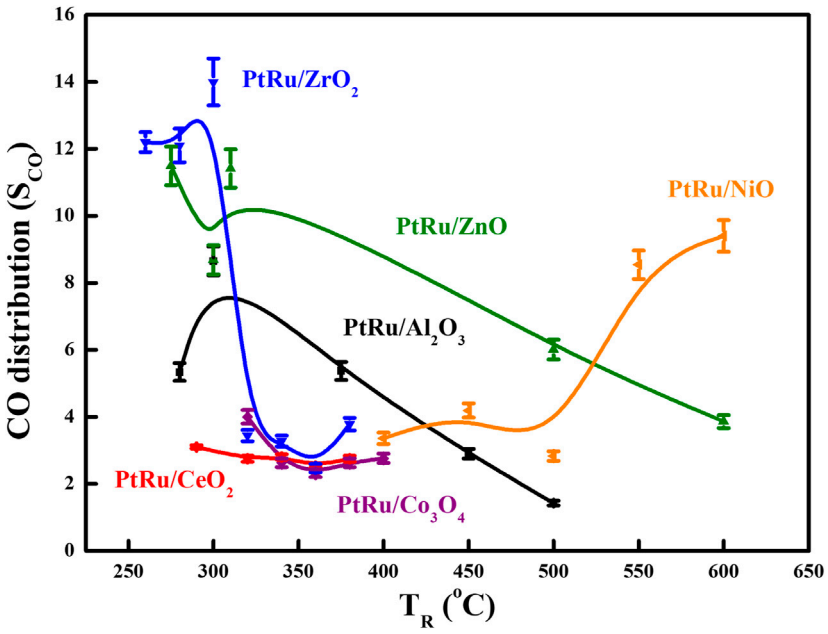

FIGURE 3
S_{CO} of series PtRu-based catalysts for OSRE reaction under various temperatures.

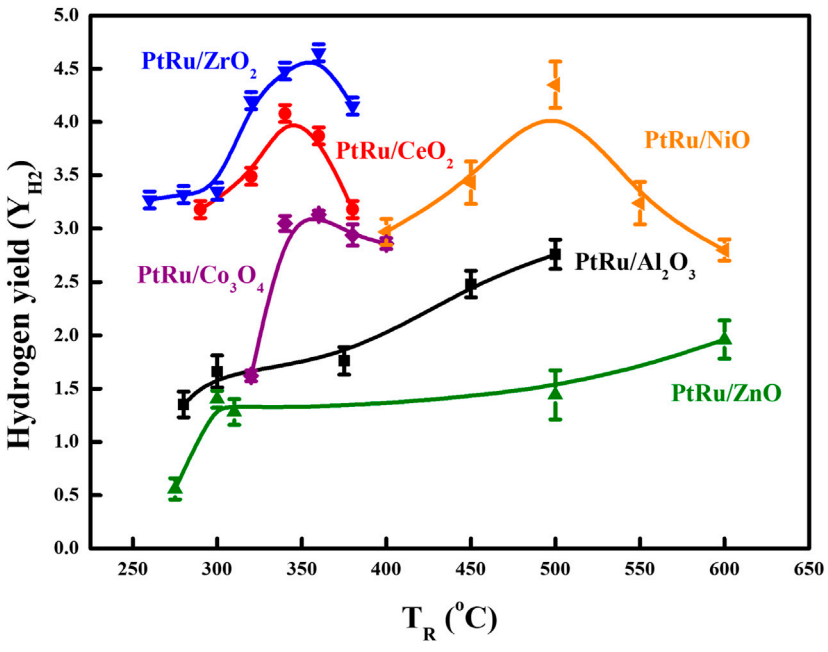

FIGURE 4
Y_{H2} of series PtRu-based catalysts for OSRE reaction under various temperatures.

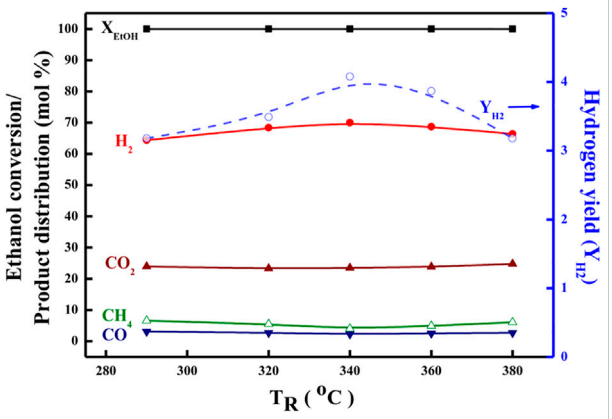

FIGURE 5
Catalytic performance in the OSRE reaction over the PtRu/CeO_2 catalyst under O_2/EtOH = 0.44, H_2O/EtOH = 4.9.

3.2 Catalytic activity of oxidative steam reforming of ethanol reaction

3.2.1 Effect of feed molar ratio

For the purpose of verification, the optimal feeds on the molar ratio of H_2O/EtOH and O_2/EtOH, the PtRu/ZrO_2 sample has been chosen to tune both H_2O/EtOH and O_2/EtOH molar ratio, separately. First, a regular H_2O/EtOH molar ratio of 4.9 was transmitted to the reactor to adjust the O_2/EtOH molar ratio (0.32, 0.44, and 0.61, respectively). All situations revealed a complete conversion at and above 300°C. The distribution of products and the hydrogen yield are displayed in Table 2, which shows that the diminishing of the O_2/EtOH ratio inclines to grow in number the amount of by-products (CO and CH_4) and lessened the hydrogen yield from 280°C to 320°C. However, the raising of the O_2/EtOH molar ratio inclines to facilitate the oxidation of hydrogen and reduced the hydrogen yield. Based on the tuning of O_2/EtOH, 0.44 was the most appropriate molar ratio. Under this circumstance, both the Y_{H2} improved and the CO reduced with the raising of the reaction temperature (T_R). Second, a definite O_2/EtOH molar ratio of 0.44 was delivered to the reactor to regulate the H_2O/EtOH molar ratio (0.8, 2.2, 4.9, and 13, respectively). The product distribution and hydrogen yield are exhibited in Table 3, which reveals that the diminishing of the H_2O/EtOH ratio inclines to boost the POE reaction, while the raising of the H_2O/EtOH ratio stimulates produce more CO side-product. According to the regulating of the H_2O/EtOH, 4.9 was the most appropriate molar ratio for the OSRE reaction, as it enhanced the hydrogen yield and reduced the CO distribution manifestly from 280°C to 320°C.

3.2.2 Effect of support

The literature (Mavrikakis and Barteau, 1998; Cavallaro et al., 2003; Fierro et al., 2005; Diagne et al., 2002) has reported that maintaining the OSRE process at a low temperature can preclude methanation (at an adequate temperature of around 500°C) and initiate large amounts of CO (at an adequate temperature of around 700°C). Based on the above consequents, the optimized feeds of the O_2/EtOH and H_2O/EtOH on the OSRE reaction were 0.44 and 4.9, respectively.

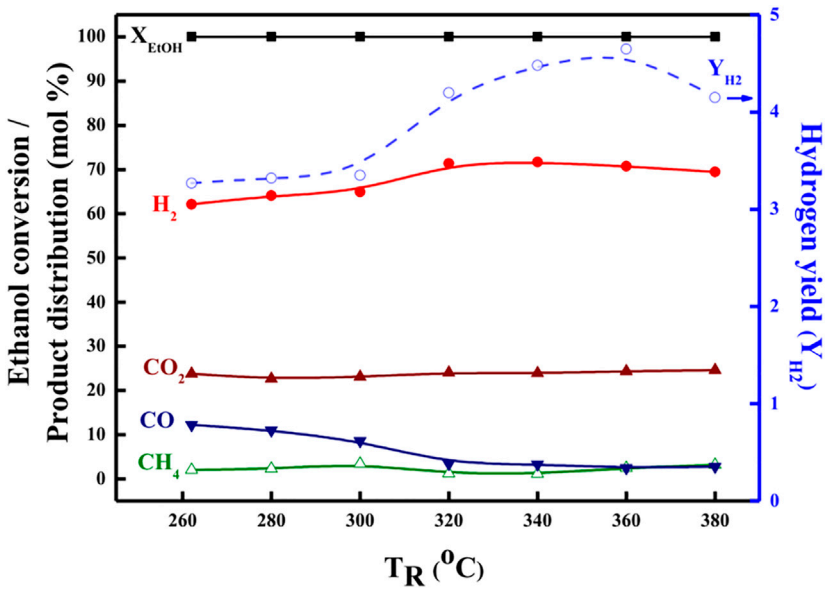

FIGURE 6
Catalytic performance in the OSRE reaction over the PtRu/ZrO_2 catalyst under O_2/EtOH = 0.44, H_2O/EtOH = 4.9.

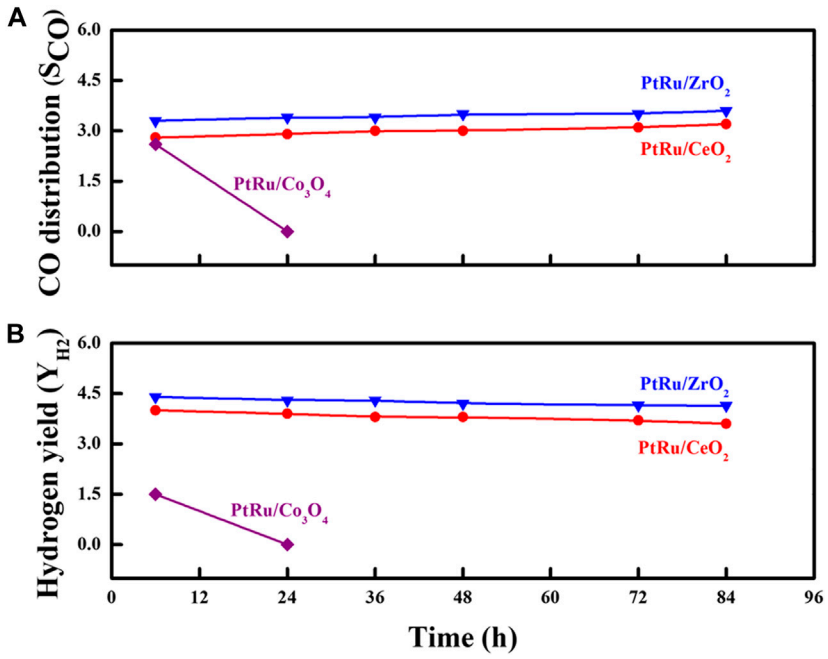

FIGURE 7
Durability test for the OSRE reaction over $PtRu/ZrO_2$, $PtRu/CeO_2$ and $PtRu/Co_3O_4$ catalysts: **(A)** S_{CO} **(B)** Y_{H2}.

Keeping this reforming condition, six bimetallic PtRu-based catalysts have been evaluated. Table 4 summarizes the conversion and distribution of products, and Figures 3, 4 gather up the Y_{H2} and S_{CO} over the series of PtRu-based catalysts for the OSRE reaction under various temperatures. The curves in Figures 3, 4 were drawn based on the fitting algorithm of the B-spline curve brought into the experimental data. In order to discuss the uncertainty analysis for numerical data, each sample was evaluated three times separately and the results indicated that the error was within ±1%–5%. Apparently, a synergistic effect emerged between the metal oxide supports and PtRu active species. The ethanol could be converted completely at lower temperatures for the reducible oxides (CeO_2 and ZrO_2 ≈ 280°C, Co_3O_4 > 300°C) supported catalysts with only C_1 species (CH_4, CO, and CO_2), while the ethanol could be converted completely at higher temperatures for the irreducible oxides (Al_2O_3 > 350°C, NiO >400°C, and ZnO >450°C) supported catalysts with C_1 species and a trace amount of undesirable C_2H_4 and CH_3CHO species. Although the catalytic activity of the $PtRu/Co_3O_4$ catalyst was bright and the S_{CO} was lower, the Y_{H2} was also lower than 3, and the long-time reaction impel a deactivation by the progressive deposited carbon. The Y_{H2} was high for the PtRu/NiO catalyst, while the T_R approached a high temperature that initiated the decomposition of ethanol and increased the S_{CO} as the T_R moved above 500°C. Both the $PtRu/Al_2O_3$ and the PtRu/ZnO catalysts possessed a lower Y_{H2} and higher S_{CO}. Bi et al. (Bi et al., 2007b) suggested that the reducible oxides could offer the lattice oxygen (O_L) to assist the oxidation of adsorbed CO (CO_{ad}), and the irreducible oxides lacked the lattice oxygen which made the oxygen molecules had to be adsorbed on the metal surface (O_{ad}). Since the O_L is more effective than O_{ad} for oxidation of CO_{ad}, therefore, a high S_{CO} produced easily from the desorption of CO_{ad} over the irreducible oxides, and the O_{ad} could integrate the adjacent adsorbed hydrogen to lower the Y_{H2}. Additionally, both the CeO_2 and the ZrO_2 can improve the dispersion of the active phase (Srinivas et al., 2003; Biswas and Kunzru, 2008), and possess large amount of surface oxygen vacancies that can restore/release oxygen (Hori et al., 1998; Silva et al., 2005) to prevent deactivation by the deposited coke and were active in the water gas shift (WGS) reaction (Gutierrez et al., 2011) to elevate the Y_{H2} and lower the S_{CO}. Both the Co_3O_4 and the NiO have been reported to exhibit the performance C–C bond cleavage on reforming of ethanol and a high Y_{H2}, however, both deactivated easily *via* the sintering and/or carbon deposition over the catalyst surface (Abdelkader et al., 2013; Sekine et al., 2009; da Silva et al., 2011). The Al_2O_3 has low mobile oxygen vacancies (Duprez, 1997), there is a limited number of oxygen intermediates available for CO oxidation, and the acidic support can stimulate the dehydration of ethanol to ethylene (Fatsikostas and Verykios, 2004), which pursued a high S_{CO} and low Y_{H2}

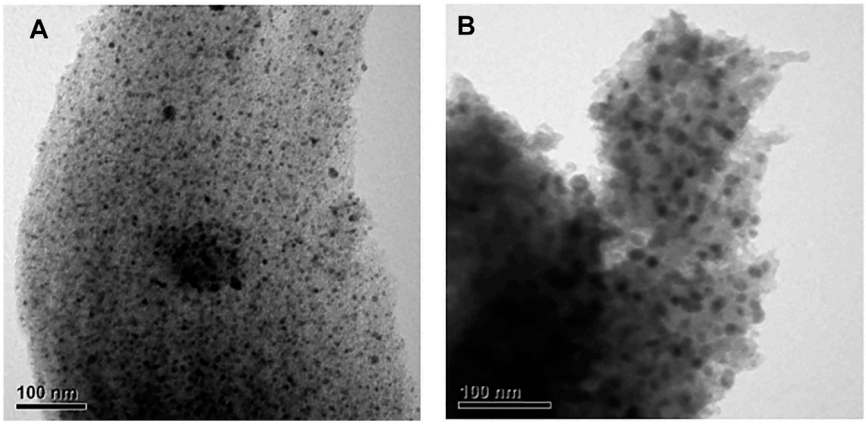

FIGURE 8
TEM images of PtRu/Co_3O_4 catalyst: **(A)** Fresh **(B)** Spent.

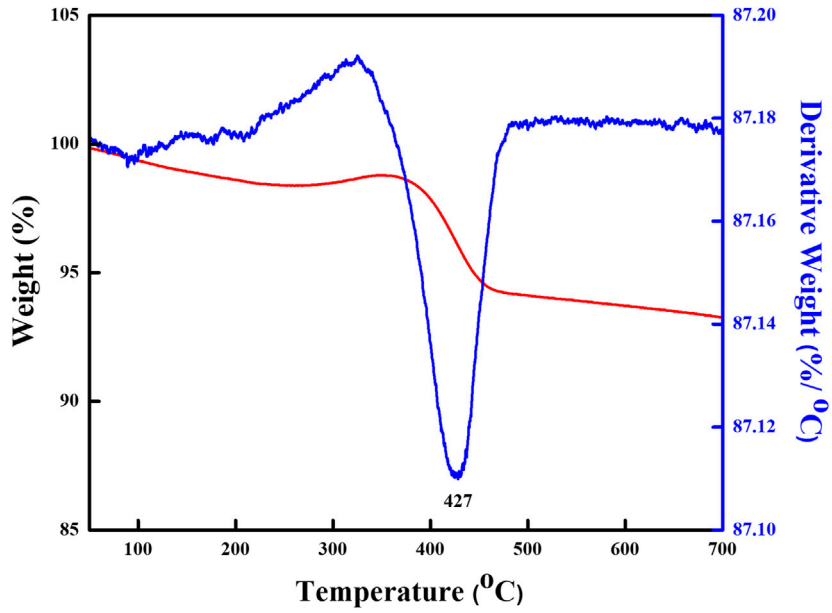

FIGURE 9
TG/DTG profiles of spent PtRu/Co_3O_4 catalyst.

production. Based on the demonstration and comparison of these reported literatures, in this study, both the PtRu/ZrO_2 and the PtRu/CeO_2 presented well-dispersed and excellent OSRE catalysts to produce hydrogen under low temperatures. The maximum Y_{H2} approached 4.5 and the S_{CO} was 3.3 mol% at 340°C for the PtRu/ZrO_2 catalyst, while the Y_{H2} was 4.0 and the CO distribution was 2.8 mol% for the PtRu/CeO_2 catalyst, respectively.

Further, in order to ascertain the features and derivations of the OSRE pathways over PtRu-based catalysts, the ethanol conversion along with the distribution of H_2, CO_2, CH_4, and CO products in the outlet stream as a function of the T_R was plotted between 260 and 380°C for both the PtRu/CeO_2 and the PtRu/ZrO_2 catalysts, as shown in Figures 5, 6. Summarizing with Table 4, also, comparing with other studies (Rabenstein and Hacker, 2008; Bi et al., 2007a; Mavrikakis and Barteau, 1998; Hung et al., 2012), the simplified

reaction network in the OSRE process over the PtRu-based catalysts was outlined in Scheme 1. The involved intermediate steps included a variety of reactions which depended on the dependency relationships of different functionalities of the catalyst. Only minor ethylene produced over the $PtRu/Al_2O_3$ catalyst *via* the dehydration of adsorbed ethanol. All catalysts showed that the ethanol could be converted completely over the whole temperature range, and the consumption of oxygen was complete. The products of the H_2 and CO_2 increased with the T_R. Thus, the performance at relatively low temperatures (<300°C) was mainly due to the partial oxidation of ethanol by consuming the O_2 according to Eq. 4:

$$C_2H_5OH + {}^3\!/_2O_2 \rightarrow 2CO_2 + 3H_2 \quad (4)$$

The key step of ethanol reforming is the cracking of the C–C bond. The C–C bond can be cracked easily through the use of ruthenium and platinum (Davda et al., 2005; Zhao et al., 2019; Rajabi et al., 2021; Zare et al., 2021). The initial partial ethanol oxidation provided the potential for the dehydrogenation of the ethanol (Eqs 5, 6) and its decarbonylation (Eq. 8) over the $PtRu/ZrO_2$ and $PtRu/CeO_2$ catalysts are quicker than PtRu/ZnO and PtRu/NiO (where * is the active site), where the later produced a minor CH_3CHO *via* desorption of adsorbed acetaldehyde.

$$C_2H_5OH + * \rightarrow CH_3CHO - * + H_2 \quad (5)$$

$$CH_3CHO - * \rightarrow CH_3CO - * + 1/2H_2 \quad (6)$$

$$CH_3CHO - * \rightarrow CH_3CHO + * \quad (7)$$

$$CH_3CO - * + * \rightarrow CO - * + CH_3 - * \quad (8)$$

The amount of CH_4 was lower on both $PtRu/ZrO_2$ and $PtRu/CeO_2$ catalysts, indicating that the sequent steam reforming of the methyl (Eq. 9) after the splitting of the acetyl group (CH_3CO) was preferential over the formation of methane (Eq. 10).

$$CH_3 - * + H_2O \rightarrow CO + 5/2H_2 \quad (9)$$

$$CH_3 - * + H - * \rightarrow CH_4 + 2* \quad (10)$$

The S_{CO} over $PtRu/CeO_2$ was lower than $PtRu/ZrO_2$ catalyst, while the CO distribution over $PtRu/ZrO_2$ declined abruptly and accompanied the increase of CO_2 and H_2 as the T_R upon 300°C. Also, the amount of CH_4 grew and accompanied the decrease of H_2 as the T_R moved above 360°C. In accordance with these observations, the $PtRu/CeO_2$ catalyst could preferentially oxidize the CO (Eq. 11) in the hydrogen-rich gases at a lower T_R. The WGS (Eq. 12) reaction was favorable compared to the $PtRu/ZrO_2$ catalyst at temperatures above 300°C for lowering the amount of CO, and the increase of CH_4 coupled with the decrease of H_2 upon 360°C was attributed to the methanation of CO or CO_2 (Eq. 13).

$$CO - *(H_2) + O - * \rightarrow CO_2(H_2) + 2* \quad (11)$$

$$CO - * + H_2O \rightarrow CO_2 + H_2 + * \quad (12)$$

$$CO - * + 3H_2 \rightarrow CH_4 + H_2O + * \quad (13)$$

3.2.3 Catalytic stability

Stability is a judgmental feature of any heterogeneous catalyst that decides its efficiency in a catalytic reaction. In order to highlight the discrepancy in the Y_{H2} and S_{CO} over the three reducible oxide-supported PtRu catalysts for the OSRE reaction, the evaluation of the catalyst stability was carried out as a function of the time-on-flux at 340°C, as shown in Figure 7. Except for the $PtRu/Co_3O_4$ catalyst, in which the activity decayed quickly with the reaction time, the conversion of the EtOH remained complete within the test over $PtRu/ZrO_2$ and $PtRu/CeO_2$ catalysts. Under the OSRE reaction, the deactivation of the Co-based catalyst could be attributed to the deposited coke, sintering of the active phase, and the encapsulation of metal sites into the support (da Silva et al., 2010; Espitia-Sibaja et al., 2017). Figure 8 displays the TEM image of the fresh and spent $PtRu/Co_3O_4$ catalyst. Apparently, the well-dispersed PtRu nanoparticles were somewhat agglomerated and capsulated by the amorphous carbon through the OSRE reaction over the $PtRu/Co_3O_4$ catalyst. To affirm the amorphous carbon, further analysis with thermal analysis, and the TG/DTG profile of spent $PtRu/Co_3O_4$ catalyst was listed in Figure 9. Apparently, the deposited carbon (~6.5%wt loss) could be oxidized around 427°C. Both the $PtRu/ZrO_2$ and $PtRu/CeO_2$ catalysts showed preferential durability and exceeded 80 h of stability, whereas the $PtRu/Co_3O_4$ catalyst was deactivated within 20 h by the deposited carbon. The maximum Y_{H2} was maintained at 4.5–4.2 and the CO distribution approached 3.3–3.5 mol% on the $PtRu/ZrO_2$ catalyst. The maximum Y_{H2} stayed at 4.0–3.6 and the CO distribution approached 2.8–3.2 mol% over the $PtRu/CeO_2$ catalyst, respectively, around 84 h test at 340. Many reactions are associated with the OSRE, the aims to pursue a high Y_{H2} while generating minimum CO. Greluk et al. (Greluk et al., 2016) studied the OSRE (H_2O:EtOH:O_2 = 9:1:0.7) using $PtKCo/CeO_2$ catalyst, the temperature of 420°C was sufficient to achieve complete conversion but only maintained 5 h. Coke deposition that led to the removal of active sites from the catalyst surface was considered to be the major deactivation mechanism. The H_2 distribution decreased from 68% to 60%, and the CO distribution increased from 2% to 2.5% with the increase of process time. Casanovas et al. (Casanovas et al., 2006) investigated the OSRE (H_2O:EtOH:O_2 = 13:1:0.5) using Pd/ZnO catalyst at low temperatures (300°C – 450°C), the ethanol could be converted completely. The H_2 selectivity increased from 37% to 61%, and the CO selectivity decreased from 4.9% to 0.1% with increasing temperature. Palma et al. (Palma et al., 2017) surveyed the OSRE on mesoporous silica supported $PteNi/CeO_2$ catalysts, which displayed stable behavior for 135 h under 500°C. Therefore, the fabricated $Pt\text{-}Ru/ZrO_2$ showed potential as a candidate OSRE catalyst under low temperatures in this study.

4 Conclusion

This investigation indicated that the feed molar ratio and kinds of support have influence on the catalytic performance of

PtRu-based catalysts. The optimal molar ratios of the H_2O/EtOH and O_2/EtOH feeds were 4.9 and 0.44, respectively for the OSRE reaction. In addition to the synergistic effect emerged between the metal oxide supports and PtRu active species, the reducible oxide supports also could provide the lattice oxygen to promote the oxidation of CO and the water gas shift reaction. Both the PtRu/ZrO_2 and the PtRu/CeO_2 catalysts appeared to be excellent OSRE catalysts to produce hydrogen under low temperatures with lesser distributions toward unwanted CO and CH_4 with complete ethanol conversion. Evidently, the PtRu supported on ZrO_2 and CeO_2 exhibited superior catalytic performance in the OSRE reaction. It was quite stable during a long time evaluation of more than 80 h; the maximum Y_{H2} was maintained at 4.5–4.2 and the CO distribution approached 3.3–3.5 mol% around 84 h test at 340°C on the PtRu/ZrO_2 catalyst.

Data availability statement

The original contributions presented in the study are included in the article/supplementary material, further inquiries can be directed to the corresponding authors.

Author contributions

C-HL: investigation, methodology, software. S-WY: investigation, methodology. C-WT: data curation, conceptualization, writing—original draft preparation. C-BW: resources, supervision, project administration, writing—review and editing.

Acknowledgments

We are pleased to acknowledge the financial support for this study from the Ministry of Science and Technology, Taiwan under contract number of MOST 108-2113-M-606-001-.

Conflict of interest

The authors declare that the research was conducted in the absence of any commercial or financial relationships that could be construed as a potential conflict of interest.

Publisher's note

All claims expressed in this article are solely those of the authors and do not necessarily represent those of their affiliated organizations, or those of the publisher, the editors and the reviewers. Any product that may be evaluated in this article, or claim that may be made by its manufacturer, is not guaranteed or endorsed by the publisher.

References

Abdelkader, A., Daly, H., Saih, Y., Morgan, K., Mohamed, M. A., Halawy, S. A., et al. (2013). Steam reforming of ethanol over Co_3O_4-Fe_2O_3 mixed oxides. *Int. J. Hydrogen Energy* 38, 8263–8275. doi:10.1016/j.ijhydene.2013.04.009

Alayoglu, S., Nilekar, A. U., Mavrikakis, M., and Eichhorn, B. (2008). Ru–Pt core–shell nanoparticles for preferential oxidation of carbon monoxide in hydrogen. *Nat. Mat.* 7, 333–338. doi:10.1038/nmat2156

Armor, J. (1999). The multiple roles for catalysis in the production of H_2. *Appl. Catal. A General* 176, 159–176. doi:10.1016/s0926-860x(98)00244-0

Bi, J. L., Hong, Y. Y., Lee, C. C., Yeh, C. T., and Wang, C. B. (2007). Novel zirconia-supported catalysts for low-temperature oxidative steam reforming of ethanol. *Catal. Today* 129, 322–329. doi:10.1016/j.cattod.2006.11.027

Bi, J. L., Hsu, S. N., Yeh, C. T., and Wang, C. B. (2007). Low-temperature mild partial oxidation of ethanol over supported platinum catalysts. *Catal. Today* 129, 330–335. doi:10.1016/j.cattod.2006.10.011

Biswas, P., and Kunzru, D. (2008). Oxidative steam reforming of ethanol over Ni/CeO_2-ZrO_2 catalyst. *Chem. Eng. J.* 136, 41–49. doi:10.1016/j.cej.2007.03.057

Casanovas, A., Llorca, J., Homs, N., Fierro, J. L. G., and de la Piscina, P. R. (2006). Ethanol reforming processes over ZnO-supported palladium catalysts: Effect of alloy formation. *J. Mol. Catal. A Chem.* 250, 44–49. doi:10.1016/j.molcata.2006.01.033

Cavallaro, S., Chiodo, V., Freni, S., Mondello, N., and Frusteri, F. (2003). Performance of Rh/Al_2O_3 catalyst in the steam reforming of ethanol: H_2 production for MCFC. *Appl. Catal. A General* 249, 119–128. doi:10.1016/s0926-860x(03)00189-3

Chiou, J. Y. Z., Wang, W. Y., Wang, C. B., and Yeh, C. T. (2012). Surface area effect of zinc oxide for steam reforming of ethanol over supported-platinum catalystsffect of zinc oxide for steam reforming of ethanol over supported-platinum catalysts. *e-J. Surf. Sci. Nanotechnol.* 10, 431–436. doi:10.1380/ejssnt.2012.431

da Silva, A. M., da Costa, L. O. O., Souza, K. R., Mattos, L. V., and Noronha, F. B. (2010). The effect of space time on Co/CeO_2 catalyst deactivation during oxidative steam reforming of ethanol. *Catal. Commun.* 11, 736–740. doi:10.1016/j.catcom.2010.02.005

da Silva, A. M., Mattos, L. V., den Breejen, J. P., Bitter, J. H., de Jong, K. P., and Noronha, F. B. (2011). Oxidative steam reforming of ethanol over carbon nanofiber supported Co catalysts. *Catal. Today* 164, 262–267. doi:10.1016/j.cattod.2010.11.013

Davda, R. R., Shabaker, J. W., Huber, G. W., Cortright, R. D., and Dumesic, J. A. (2005). A review of catalytic issues and process conditions for renewable hydrogen and alkanes by aqueous-phase reforming of oxygenated hydrocarbons over supported metal catalysts. *Appl. Catal. B Environ.* 56, 171–186. doi:10.1016/j.apcatb.2004.04.027

de la Piscina, P. R., and Homs, N. (2008). Use of biofuels to produce hydrogen (reformation processes). *Chem. Soc. Rev.* 37, 2459–2467. doi:10.1039/b712181b

Diagne, C., Idriss, H., and Kiennemann, A. (2002). Hydrogen production by ethanol reforming over Rh/CeO_2–ZrO_2 catalysts. *Catal. Commun.* 3, 565–571. doi:10.1016/s1566-7367(02)00226-1

Duprez, D. (1997). Study of surface mobility by isotopic exchange: Recent developments and perspectives. *Stud. Surf. Sci. Catal.* 112, 13–28.

Espitia-Sibaja, M., Muñoz, M., Moreno, S., and Molina, R. (2017). Effects of the cobalt content of catalysts prepared from hydrotalcites synthesized by ultrasound-assisted coprecipitation on hydrogen production by oxidative steam reforming of ethanol (OSRE). *Fuel* 194, 7–16. doi:10.1016/j.fuel.2016.12.086

Fatsikostas, A. N., and Verykios, X. E. (2004). Reaction network of steam reforming of ethanol over Ni-based catalysts. *J. Catal.* 225, 439–452. doi:10.1016/j.jcat.2004.04.034

Fierro, V., Akdim, O., Provendier, H., and Mirodatos, C. (2005). Ethanol oxidative steam reforming over Ni-based catalysts. *J. Power Sources* 145, 659–666. doi:10.1016/j.jpowsour.2005.02.041

Furtado, A. C., Alonso, C. G., Cantão, M. P., and Fernandes-Machado, N. R. C. (2009). Bimetallic catalysts performance during ethanol steam reforming: Influence of support materialsfluence of support materials. *Int. J. Hydrogen Energy* 34, 7189–7196. doi:10.1016/j.ijhydene.2009.06.060

Goldemberg, J. (2007). Ethanol for a sustainable energy future. *Science* 315, 808–810. doi:10.1126/science.1137013

Greluk, M., Słowik, G., Rotko, M., and Machocki, A. (2016). Steam reforming and oxidative steam reforming of ethanol over PtKCo/CeO_2 catalyst. *Fuel* 183, 518–530. doi:10.1016/j.fuel.2016.06.068

Gutierrez, A., Karinen, R., Airaksinen, S., Kaila, R., and Krause, A. O. I. (2011). Autothermal reforming of ethanol on noble metal catalysts. *Int. J. Hydrogen Energy* 36, 8967–8977. doi:10.1016/j.ijhydene.2011.04.129

Hori, C. E., Permana, H., Simon Ng, K. Y., Brenner, A., More, K., Rahmoeller, K. M., et al. (1998). Thermal stability of oxygen storage properties in a mixed CeO_2-ZrO_2 system. *Appl. Catal. B Environ.* 16, 105–117. doi:10.1016/s0926-3373(97)00060-x

Hsia, Y. Y., Huang, Y. C., Zheng, H. S., Lai, Y. L., Hsu, Y. J., Luo, M. F., et al. (2019). Effects of O_2 and H_2O in the oxidative steam-reforming reaction of ethanol on Rh catalysts. *J. Phys. Chem. C* 123, 11649–11661. doi:10.1021/acs.jpcc.9b00747

Hung, C. C., Chen, S. L., Liao, Y. K., Chen, C. H., and Wang, J. H. (2012). Oxidative steam reforming of ethanol for hydrogen production on M/Al_2O_3. *Int. J. Hydrogen Energy* 37, 4955–4966. doi:10.1016/j.ijhydene.2011.12.060

Koh, A. C. K., Chen, L., Leong, K. W., Ang, T. P., Johnson, B. F. G., Khimyak, T., et al. (2009). Ethanol steam reforming over supported ruthenium and ruthenium–platinum catalysts: Comparison of organometallic clusters and inorganic salts as catalyst precursors. *Int. J. Hydrogen Energy* 34, 5691–5703. doi:10.1016/j.ijhydene.2009.05.044

Lai, T. L., Lee, C. C., Wu, K. S., Shu, Y. Y., and Wang, C. B. (2006). Microwave-enhanced catalytic degradation of phenol over nickel oxide. *Appl. Catal. B Environ.* 68, 147–153. doi:10.1016/j.apcatb.2006.07.023

Li, D., Li, X. Y., and Gong, J. L. (2016). Catalytic reforming of oxygenates: State of the art and future prospects. *Chem. Rev.* 116, 11529–11653. doi:10.1021/acs.chemrev.6b00099

Lin, H. K., Chiu, H. C., Tsai, H. C., Chien, S. H., and Wang, C. B. (2003). Synthesis, characterization and catalytic oxidation of carbon monoxide over cobalt oxide. *Catal. Lett.* 88, 169–174.

Llorca, J., Homs, N., Sales, J., and de la Piscina, P. R. (2002). Efficient production of hydrogen over supported cobalt catalysts from ethanol steam reformingficient production of hydrogen over supported cobalt catalysts from ethanol steam reforming. *J. Catal.* 209, 306–317. doi:10.1006/jcat.2002.3643

Mavrikakis, M., and Barteau, M. A. (1998). Oxygenate reaction pathways on transition metal surfaces. *J. Mol. Catal. A Chem.* 131, 135–147. doi:10.1016/s1381-1169(97)00261-6

Ni, M., Leung, D. Y. C., and Leung, M. K. H. (2007). A review on reforming bio-ethanol for hydrogen production. *Int. J. Hydrogen Energy* 32, 3238–3247. doi:10.1016/j.ijhydene.2007.04.038

Palma, V., Ruocco, C., Meloni, E., and Ricca, A. (2017). Oxidative steam reforming of ethanol on mesoporous silica supported Pt-Ni/CeO_2 catalysts. *Int. J. Hydrogen Energy* 42, 1598–1608. doi:10.1016/j.ijhydene.2016.05.071

Pereira, E. B., de la Piscina, P. R., Martí, S., and Homs, N. (2010). H_2 production by oxidative steam reforming of ethanol over K promoted Co-Rh/CeO_2-ZrO_2 catalysts. *Energy Environ. Sci.* 3, 487–493. doi:10.1039/b924624j

Pereira, E. B., Homs, N., Martí, S., Fierro, J. L. G., and de la Piscina, P. R. (2008). Oxidative steam-reforming of ethanol over Co/SiO_2, Co–Rh/SiO_2 and Co–Ru/SiO_2 catalysts: Catalytic behavior and deactivation/regeneration processes. *J. Catal.* 257, 206–214. doi:10.1016/j.jcat.2008.05.001

Rabenstein, G., and Hacker, V. (2008). Hydrogen for fuel cells from ethanol by steam-reforming, partial-oxidation and combined auto-thermal reforming: A thermodynamic analysis. *J. Power Sources* 185, 1293–1304. doi:10.1016/j.jpowsour.2008.08.010

Rajabi, Z., Jones, L., Martinelli, M., Qian, D., Cronauer, D. C., Kropf, A. J., et al. (2021). Influence of Cs promoter on ethanol steam-reforming selectivity of Pt/m-ZrO_2 catalysts at low temperature. *Catalysts* 11, 1104. doi:10.3390/catal11091104

Ramachandran, R., and Menon, R. K. (1998). An overview of industrial uses of hydrogen. *Int. J. Hydrogen Energy* 23, 593–598. doi:10.1016/s0360-3199(97)00112-2

Sekine, Y., Kazama, A., Izutsu, Y., Matsukata, M., and Kikuchi, E. (2009). Steam reforming of ethanol over cobalt catalyst modified with small amount of iron. *Catal. Lett.* 132, 329–334. doi:10.1007/s10562-009-0133-6

Siang, J. Y., Lee, C. C., Wang, C. H., Wang, W. T., Deng, C. Y., Yeh, C. T., et al. (2010). Hydrogen production from steam reforming of ethanol using a ceria-supported iridium catalyst: Effect of different ceria supports. *Int. J. Hydrogen Energy* 35, 3456–3462. doi:10.1016/j.ijhydene.2010.01.067

Silva, P. P., Silva, F. A., Portela, L. S., Mattos, L. V., Noronha, F. B., and Hori, C. E. (2005). Effect of Ce/Zr ratio on the performance of Pt/$CeZrO_2$/Al_2O_3 catalysts for methane partial oxidation. *Catal. Today* 107, 734–740. doi:10.1016/j.cattod.2005.07.004

Srinivas, D., Satyanarayana, C. V. V., Potdar, H. S., and Ratnasamy, P. (2003). Structural studies on NiO-CeO_2-ZrO_2 catalysts for steam reforming of ethanol. *Appl. Catal. A General* 246, 323–334. doi:10.1016/s0926-860x(03)00085-1

Tóth, M., Varga, E., Oszkó, A., Baán, K., Kiss, J., and Erdőhelyi, A. (2016). Partial oxidation of ethanol on supported Rh catalysts: Effect of the oxide support. *J. Mol. Catal. A Chem.* 411, 377–387. doi:10.1016/j.molcata.2015.11.010

Trovarelli, A. (1996). Catalytic properties of ceria and CeO_2-containing materials. *Catal. Rev.* 38, 439–520. doi:10.1080/01614949608006464

Wang, C. B., Gau, G. Y., Gau, S. J., Tang, C. W., and Bi, J. L. (2005). Preparation and characterization of nanosized nickel oxide. *Catal. Lett.* 101, 241–247. doi:10.1007/s10562-005-4899-x

Wang, C. B., Tang, C. W., Gau, S. J., and Chien, S. H. (2005). Effect of the surface area of cobaltic oxide on carbon monoxide oxidation. *Catal. Lett.* 101, 59–63. doi:10.1007/s10562-004-3750-0

Wang, C. H., Ho, K. F., Chiou, J. Y. Z., Lee, C. L., Yang, S. Y., Yeh, C. T., et al. (2011). Oxidative steam reforming of ethanol over PtRu/ZrO_2 catalysts modified with sodium and magnesium. *Catal. Commun.* 12, 854–858. doi:10.1016/j.catcom.2011.02.002

Wang, Z., and Spivey, J. J. (2015). Effect of ZrO_2, Al_2O_3 and La_2O_3 on cobalt-copper catalysts for higher alcohols synthesis. *Appl. Catal. A General* 507, 75–81. doi:10.1016/j.apcata.2015.09.032

Youn, M. H., Seo, J. G., Lee, H., Bang, Y., Chung, J. S., and Song, I. K. (2010). Hydrogen production by auto-thermal reforming of ethanol over nickel catalysts supported on metal oxides: Effect of support acidity. *Appl. Catal. B Environ.* 98, 57–64. doi:10.1016/j.apcatb.2010.05.002

Zanchet, D., Santos, J. B. O., Damyanova, S., Gallo, J. M. R., and Bueno, J. M. C. (2015). Toward understanding metal-catalyzed ethanol reforming. *ACS Catal.* 5, 3841–3863. doi:10.1021/cs5020755

Zare, M., Saleheen, M., Zare, M., Saleheen, M., Mamun, O., Heyden, A., et al. (2021). Aqueous-phase effects on ethanol decomposition over Ru-based catalysts. *Catal. Sci. Technol.* 11, 6695–6707. doi:10.1039/d1cy01057c

Zhang, R. J., Xia, G. F., Li, M. F., Wu, Y., Nie, H., and Li, D. D. (2015). Effect of support on the performance of Ni-based catalyst in methane dry reforming. *J. Fuel Chem. Technol.* 43, 1359–1365. doi:10.1016/s1872-5813(15)30040-2

Zhao, Z., Zhang, L., Tan, Q. H., Yang, F. F., Faria, J., and Resasco, D. (2019). Synergistic bimetallic Ru–Pt catalysts for the low-temperature aqueous phase reforming of ethanol. *AIChE J.* 65, 151–160. doi:10.1002/aic.16430